Vol. 62: 241–250, 2015
doi: 10.3354/cr01271

CLIMATE RESEARCH
Clim Res

Published online February 5

Dendroclimatic reconstruction of temperature in the eastern Qilian Mountains, northwestern China

Linlin Gao[1], Xiaohua Gou[1,2,*], Yang Deng[1], Meixue Yang[3], Fen Zhang[1], Jin Li[1]

[1]MOE Key Laboratory of Western China's Environmental Systems, Collaborative Innovation Centre for Arid Environments and Climate Change, Lanzhou University, Lanzhou 73000, PR China
[2]Tree-Ring Laboratory, Lanont-Doherty Earth Observatory of Columbia University, 61 Route 9W, Palisades, NY 10964, USA
[3]State Key Laboratory of Cryospheric Sciences, Cold and Arid Regions Environmental and Engineering Research Institute, Chinese Academy of Sciences, Lanzhou 730000, PR China

ABSTRACT: Understanding the extent to which climate has varied in the past is a prerequisite to assessing current trends. In this study, we present a 225 yr tree-ring width record of Qinghai spruce *Picea crassifolia* from a mesic site in the eastern Qilian Mountains of northwest China. This tree-ring record showed significant positive correlations ($p < 0.05$) with temperature for most months from the preceding May to the current September, but none with precipitation or the Palmer Drought Severity Index. Based on the correlation relationships, we developed a regression model to reconstruct the average July temperatures over the period AD 1785–2009, which accounted for 45% of the observed temperature variation during the calibration period (1957–2009). This is the first tree-ring based temperature reconstruction in the eastern Qilian Mountains. The reconstruction indicated a warming trend that began around 1900 and continued through the late 20th century. Eight of the 10 warmest years were recorded during the period 1990–2009. The longest cool period occurred in 1894–1916. Comparisons of our reconstruction with other independent tree-ring based temperature reconstructions from the northeastern Tibetan Plateau suggest coherent variance patterns in these warm season temperature reconstructions regardless of the positive or negative correlation relationships between tree-ring records and temperatures. The results of comparisons also indicated that the warm season temperature variances lag behind the winter temperature variability by about 20 yr in this region.

KEY WORDS: Tree-ring · Temperature reconstruction · Warming trend · *Picea crassifolia* · Northwest China

1. INTRODUCTION

Global mean surface temperature has increased significantly during the past several decades, accompanied by high atmospheric CO_2 concentrations (IPCC 2013). To understand whether the recent warming is unusual and can be attributed to anthropogenic activities, it is necessary to place the recent changes into a long-term climatic context. Paleoclimate reconstructions have been carried out in many areas of the world as they can supply information on past climate variations via paleoclimatic archives, such as tree-ring records. However, differences can be expected among regions because some areas are warming dramatically (Vaughan et al. 2003), while others exhibit no trend or show cooling (Doran et al. 2002, Easterling & Wehner 2009). Therefore, regional climate variation research is essential for improving our understanding of recent climate change as well as providing basal data for large-scale climate change studies.

The Qilian Mountains are located at the northeastern margin of the Tibetan Plateau in northwest China. The region is characterized by low precipitation and

*Corresponding author: xhgou@lzu.edu.cn

relatively high mountainous terrain. As the harsh climatic conditions limit tree growth rates, numerous old trees have been found here. Many dendroclimatic studies based on the tree-ring materials have been conducted in the region (e.g. Liu et al. 2010, Yang et al. 2011, Deng et al. 2013). However, most previous studies focused on precipitation, Palmer Drought Severity Index (PDSI), or streamflow reconstructions (e.g. Fang et al. 2009, Sun & Liu 2012, Chen et al. 2013). Several attempts to reconstruct past temperature variations for the northeastern Tibetan Plateau have been made based on the inverse relationships between tree-ring chronologies and temperature (Tian et al. 2009, Chen et al. 2012). However, tree-ring records which are positively correlated with temperatures are still scarce in this region (Gou et al. 2007, Zhu et al. 2008). The directly correlated effects of temperature on tree growth (e.g. direct temperature effects on physiological processes and photosynthetic rates) are likely to produce a more reliable expression of past temperature variability compared to inversely correlated temperature effects on growth, which are more likely related to moisture stress (Cook et al. 2013a). To clarify this and to provide a new climatic record, we looked for tree-ring records from a region in the eastern Qilian Mountains where drought is less common and a trend in rising temperature would generally favor increased rather than decreased tree growth.

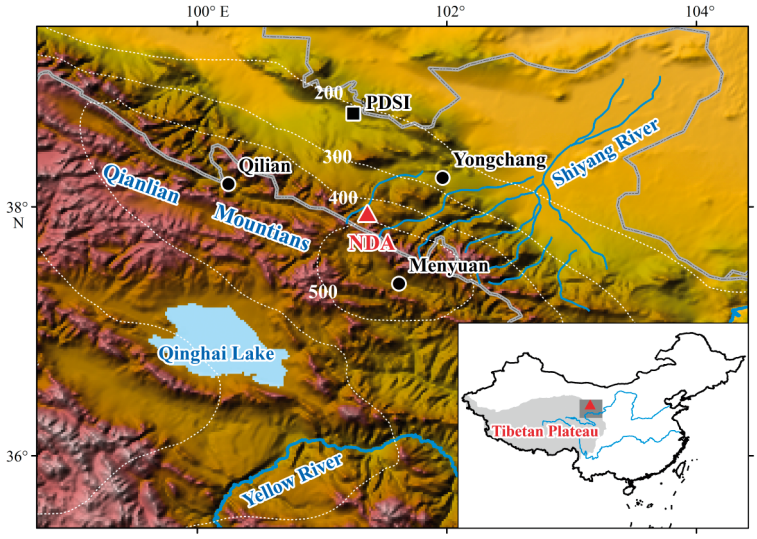

Fig. 1. Study region showing the study site (NDA, red triangle) and nearby meteorological stations (Yongchang, Qilian, and Menyuan, black dots) and Palmer Drought Severity Index (PDSI) grid (black square). Dotted white lines: mean annual precipitation (100 mm yr^{-1} contours) estimated by the Tropical Rainfall Measuring Mission (TRMM) satellite for the period 1998–2012 (Huffman et al. 2007)

Our objective in this study was to present the first tree-ring based temperature reconstruction using Qinghai spruce ring-width data from the eastern Qilian Mountains. We also examined whether there is any difference between positive and negative correlation based temperature reconstructions by comparing the resulting reconstruction with independently derived tree-ring based temperature reconstructions. Additionally, we examined the features of temperature variability in different seasons in the study area.

2. DATA AND METHODS

2.1. Study area

The study area is situated in the Shiyang River basin in the eastern part of the Qilian Mountains (Fig. 1), where the transition between semi-arid and arid climate zones occurs. Seasonal climate variation here is influenced by the East Asian monsoon, the westerly circulation, and the Siberian High (Wang et al. 2006). The precipitation contour lines in Fig. 1 show a sharp north to south precipitation gradient from <200 mm to >500 mm per annum. The nearest 3 meteorological stations to our sampling site are Qilian, Menyuan, and Yongchang stations. The Qilian and Menyuan stations are situated in the mountainous area, while the Yongchang station lies outside the mountainous region (Fig. 1). The annual average temperatures from AD 1957–2009 were 0.8°C for the Qilian station and 1.0°C for the Menyuan station, and the mean annual total precipitation for these stations was 525 mm and 406 mm, respectively. In contrast, the climatic conditions at the Yongchang station (1959–2009) are warmer and drier, with a mean annual temperature of 5.1°C and a mean annual total precipitation of 201 mm. Thus the climatic conditions are notably divergent in different parts of the eastern Qilian Mountains. Our sampling site is close to the regional rainfall center, with annual total precipitation at about 500 mm (Fig. 1). The temperature and precipitation in this region follow a strong seasonal pattern, with the highest temperatures and most of the precipitation recorded during the summer. The peaks for temperature and precipitation are generally in July (Fig. 2). The dominant tree is Qinghai spruce, which generally grows on

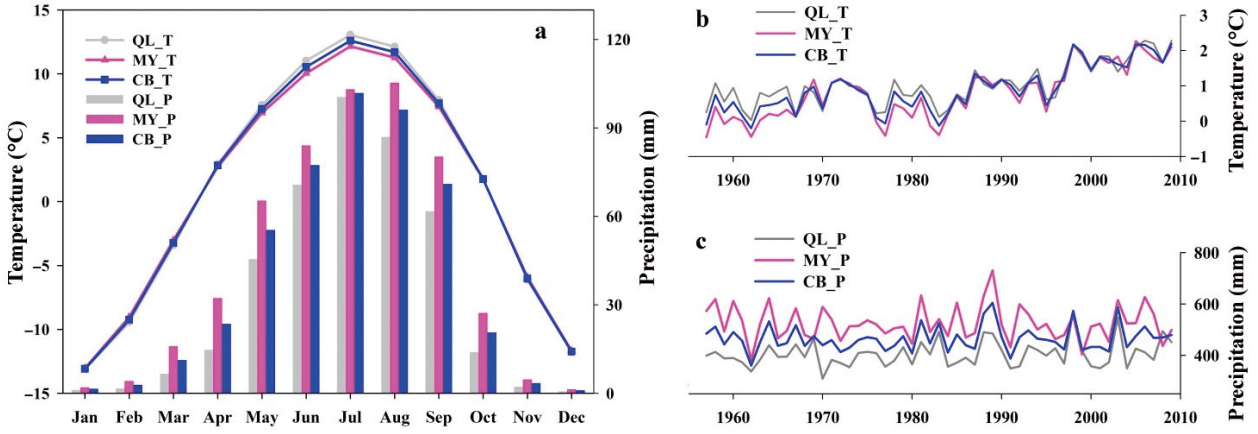

Fig. 2. (a) Monthly mean temperature (T, lines) and total precipitation (1957–2009; P, bars) from the Qilian (QL) and Menyuan (MY) meteorological stations, and the combined climate data (CB) from these 2 stations. (b,c) Time series plots of (b) mean annual temperature and (c) precipitation for the period 1957–2009 from Qilian, Menyuan, and combined climate data

shaded slopes. *Salix oritrepha* C.K. Schneid., *Caragana jubata* (Pall.) Poir, and *Potentilla fruticosa* are common shrubs growing in light gaps, while *Stipa bungeana* Trin. and *S. breviflora* Griseb are the most common grasses and *Achnatherum splendens* (Trin.) Nevski is the most common herb growing under forest cover (Cheng et al. 2004).

2.2. Tree-ring data

We collected tree ring samples from a Qinghai spruce forest ranging in elevation from 3190 to 3210 m a.s.l. The sampling site (hereafter NDA) is situated on a gentle slope with relatively deep soils. This site represents an open mono-species stand of Qinghai spruce with prevailing old trees and low competitive effects. One or 2 increment cores were extracted at breast height (approximately 1.3 m above ground level) from each individual tree, and a total of 52 increment cores from 27 trees were collected. All samples were taken to the laboratory and processed according to standard techniques of dendrochronology (Stokes & Smiley 1968). Cores were first air-dried, mounted, and sanded. The tree-ring series were then dated under the microscope with visual cross-dating. Finally, ring-widths were measured using the Velmex measuring system with a precision of 0.001 mm. The quality of cross-dating was further checked using the TSAP and COFECHA programs (Holmes 1983, Rinn 2003). The cross-dating results suggested no absent rings, and the interannual variation for these tree-ring series was very consistent, with a mean series intercorrelation of 0.65. As a result of the good cross correlations, all of the ring-width series were utilized to develop the final chronology.

To eliminate the age-related trends in the raw ring-width series as well as to preserve low-frequency signals, conventional straight lines or negative exponential curves were applied for detrending. The tree-ring indices were calculated as ratios between ring-width measurements and the curve-fitted values. The signal-free version of the computer program ARSTAN was used to calculate tree-ring chronology (Cook et al. 2013b) (Fig. 3a). Signal-free methods are useful for mitigating trend distortion in conservative standardization methods, as the medium-frequency variance in the common climate-related forcing of tree growth can bias the removal of supposed 'non-climate' variance (Melvin & Briffa 2008).

2.3. Climate data

The monthly precipitation and mean temperature data from the Qilian and Menyuan meteorological stations were used in this study, as these 2 stations are close to our sampling site, and the elevations and climatic conditions are similar to those at the sampling site (Table 1). Considering that some tree-ring records are more sensitive to PDSI variation than to precipitation (e.g. Fang et al. 2009, Deng et al. 2013, Gao et al. 2013a), we also calculated the correlations of tree-ring chronology with the nearest PDSI grid data (38° 45′ N, 101° 15′ E, 1957–2009, Dai et al. 2004). Fig. 2 shows the monthly mean temperatures and total precipitation and the associated interannual variability for the period 1957–2009. Due to their close geographic proximity, the temperature and precipitation data from the 2 stations were combined into 1 series to represent the regional climatic conditions. To minimize the effect of differing means and

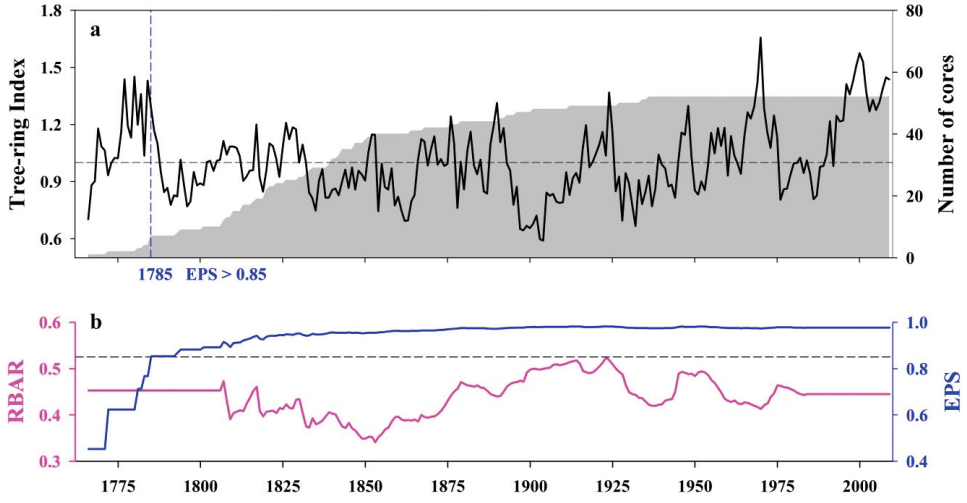

Fig. 3. (a) Ring-width chronology (black line) and sample size (number of cores, grey area). Tree-ring indices were calculated as ratios between ring-width measurements and the curve-fitted values. Horizontal dashed line: mean tree-ring index, 1766–2009; vertical dashed line: first year of expressed population signal (EPS) > 0.85. (b) Inter-series correlation coefficient (RBAR) and EPS with 51 yr window running and 1 yr step

Table 1. Location, elevation, and time span of the data record for the study site (slope: 20–30°; aspect: northeast; trees sampled: 27; cores: 52) and nearest meteorological stations and Palmer Drought Severity Index (PDSI) grid

Site	Coordinates	Elevation (m)	Time span
Study site	37° 56′ 51″ N, 101° 21′ 41″ E	3190–3210	1766–2009
Qilian station	38° 11′ N, 100° 15′ E	2787	1957–2009
Menyuan station	37° 23′ N, 101° 37′ E	2850	1957–2009
PDSI	38° 45′ N, 101° 15′ E		1957–2009

variances in the 2 records, the climate data were *z*-transformed before averaging. Both the mean and variance of the new series were converted back to the averaged values of means and standard deviations of the original monthly series (Jones & Hulme 1996). The variation patterns between the combined climate data and the original climate records are very consistent, suggesting an apparent warming trend over the past 20 yr (Fig. 2). We used the combined climate data for further analyses.

2.4. Methods of reconstruction and analysis

The expressed population signal (EPS) and mean inter-series correlation coefficient (RBAR) with a 51 yr window running and 50 yr overlaps between adjacent windows were computed to assess the common signal representativeness of the chronology (Fig. 3b). The EPS was also used as a measure of sufficient sample replication where 0.85 has been suggested to be a reasonable level (Wigley et al. 1984). Pearson correlation analyses between tree-ring chronology and climate data were applied to identify the climate–growth relationships. To account for conditions in the previous year, we calculated the correlations between the tree-ring chronology and monthly mean temperatures, precipitation and PDSI for an 18 mo period, starting with the previous May and extending to October in the year when the last cells in a selected growth ring were formed. A split-period calibration and verification method was applied to evaluate the regression model for reconstruction (Cook & Kairiukstis 1990). The strength of calibrations during the verification period was evaluated via the variance explained (R^2), sign test, *F*-test, reduction of error (RE), and the coefficient of efficiency (CE) statistics, whereby positive RE and CE values indicate a robust verification (Fritts 1976). Multitaper method (MTM) spectral analysis was used to evaluate the periodic features of the reconstruction (Mann & Lees 1996).

3. RESULTS

3.1. Correlations between tree-ring chronology and climate variables

Fig. 4 shows the correlations between tree-ring chronology and climate variables (mean temperature, precipitation, and PDSI) for the period 1957–2009. There were consistent positive correlations with temperature for both the previous and current year, with significant ($p < 0.05$) correlations in the growing season (May–September, excepting the preceding August). Positive correlations with winter temperatures

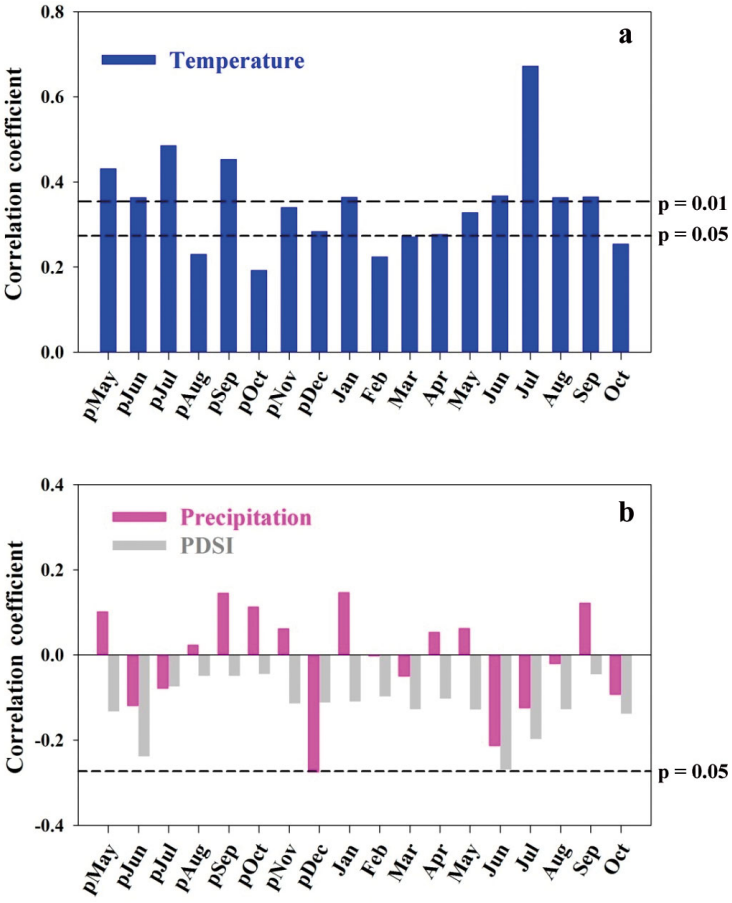

Fig. 4. Correlations between tree-ring chronology and (a) monthly mean temperature and (b) monthly precipitation and Palmer Drought Severity Index (PDSI) from May in the previous year (pMay) to October in the current growth year (Oct) for the period 1957–2009. Horizontal dashed lines: 95% (short dash) and 99% (medium dash) levels of significance. Note differences in *y*-axis scales between panels

(November–January) were also significant ($p < 0.05$). The strongest correlation was with current July temperature ($r = 0.67$, $p < 0.01$). Except for the preceding December, there were no significant ($p < 0.05$) correlations between tree-ring chronologies and precipitation. Furthermore, the correlations with PDSI were consistently negative but not significant ($p < 0.05$) for the previous and current growing year. Overall, the correlations between tree-ring chronology and climate variables indicate that tree growth at the study site is primarily a response to temperature variance, and there were no significant correlations with precipitation and PDSI. We also calculated the correlations between tree-ring chronology and the temperatures of various seasons. The highest correlation coefficient with seasonal temperature was found from June–July ($r = 0.605$), which is much lower than that of July ($r = 0.669$). Therefore, we decided to reconstruct the July temperature in this study.

3.2. July temperature reconstruction since 1785

Based on the high correlation between tree-ring chronology and July temperature, we developed a linear regression model for July temperature reconstruction:

$$T_{\text{July}} = 2.877 \times X_t + 9.236 \quad (1)$$

where T_{July} is the mean temperature in July and X_t is the tree-ring width index for that year. The correlation coefficient of the regression function is 0.67 ($n = 53$, $p < 0.01$). The reconstructed temperatures account for 44.8% (the adjusted explained variance $R^2_{\text{adj}} = 43.7\%$, $F = 41.35$) of the instrumental temperature variances over the calibration period 1957–2009. The standard deviations for the observed and reconstructed temperatures over 1957–2009 are 0.91 and 0.61, respectively. Comparisons between the reconstructed and observed July mean temperature suggest that the reconstructed temperature patterns were closely in agreement with those measured for the past several decades at both decadal and annual time steps (Fig. 5a). The split-period calibration and verification results (Table 2) indicated that the correlation coefficients were relatively high, and the sign tests were all statistically significant at the 0.05 level for both periods. The values of RE and CE were also positive for both periods. These results confirm that the regression model is good enough for reconstruction. By calculating the running correlations between tree-ring chronology and July temperatures (not shown), we confirmed that the climate-growth relationships were stable over the calibration-verification period.

Fig. 5b presents the reconstructed July mean temperature based on the linear regression model (Eq. 1) and the 10 yr low-pass filter curve over the period 1785–2009. The mean ± SD July temperature for this period is estimated at 12.1 ± 0.55°C. The 10 highest temperature years in July over the past 225 yr were 1969, 1970, 1996, 1998, 1999, 2000, 2001, 2007, 2008, and 2009, and the 10 coldest years in July occurred in 1862, 1897, 1898, 1899, 1900, 1901, 1903, 1904, 1928, and 1932. From these analyses, the 1890s and early 1900s were extremely cold compared to the long-term average, while the warmest temperatures have all occurred in the last 2 decades. If we define a warm or cool period as one with a continually higher or lower filtered value over a decade from the mean filtered curve, there were 5 warm and 6 cool periods over the past 225 yr.

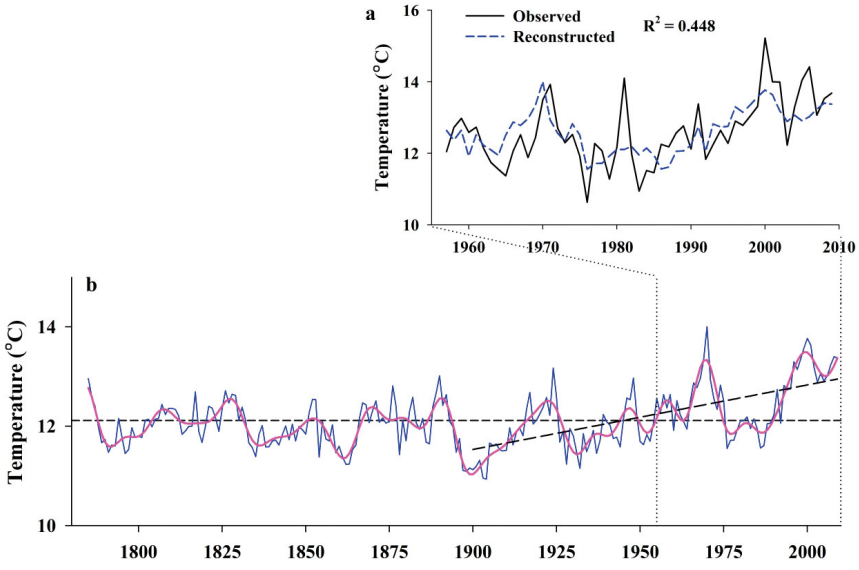

Fig. 5. (a) Comparison of observed (solid line) and reconstructed (dashed line) July mean temperature for the calibration period over the period 1957–2009. (b) July mean temperature reconstruction (blue line) and the value using a decadal low-pass filter (red line) for 1785–2009. Horizontal dashed line represents the mean of reconstructed temperature over the past 225 yr. The bias dashed line is the trend line of reconstructed temperature over 1900–2009 to highlight the temperature increase during the recent century

Table 2. Calibration and verification statistics for the July mean temperature reconstruction model. ST: signal test; RE: reduction of error; CE: coefficient of efficiency. Asterisks indicate confidence levels (**99%; *95%)

Calibration				Verification				
Period	r	R^2	*F*	Period	r	RE	CE	ST
1957–1980	0.596	0.355	12.12**	1981–2009	0.681	0.454	0.221	17+/6–*
1981–2009	0.681	0.474	25.23**	1957–1980	0.596	0.442	0.027	24+/6–**
1957–2009	0.669	0.448	41.35**					

The 5 warm periods occurred in: 1822–1831, 1867–1880, 1917–1926, 1964–1974, and 1990–2009, while the 6 cool periods were: 1788–1803, 1832–1850, 1854–1866, 1894–1916, 1927–1943, and 1975–1989. Since the early 1900s, our reconstruction shows a linear increase in July temperature with a slope of 0.13°C decade^{-1}. Between 1990 and 2000, the rate was 1.47°C decade^{-1}, after which the rate of increase declined slightly. The increasing trend of temperature was reflected by the instrumental records over the past 5 decades with a warming rate of 0.28°C decade^{-1} (Fig. 2b), which is slightly higher than our reconstruction. The rate of temperature increase from the instrumental records for 1990–2000 was 1.84°C decade^{-1}, which is also higher than that of our reconstruction.

3.3. Spectral analyses

The MTM spectral analysis (Mann & Lees 1996) was performed to evaluate the main spectral properties of the reconstructed temperature time series for the period 1785–2009 (Fig. 6). There were several significant ($p < 0.05$) interannual and interdecadal cycles in the temperature variability during the past 225 yr. The significant ($p < 0.05$) interannual power peaks at 2.1–3.8 yr fall within the range of El Niño-Southern Oscillation (ENSO) variability (Li et al. 2011). The spectral peak at 46.5 yr was also significant at the 0.05 level.

4. DISCUSSION

4.1. Climate–growth relationships

An array of tree-ring records from the northeastern Tibetan Plateau shows positive correlations with precipitation or PDSI, as well as negative correlations with temperature. Based on these tree-ring records, a number of hydroclimate reconstructions have been presented for this area (e.g. Liang et al. 2009, Qin et al. 2010, Shao et al. 2010, Fang et al. 2011, Gou et al. 2014). The tree growth response to hydroclimatic variability is closely related to xeric conditions in the inland arid region. Additionally, there are also some tree-ring based temperature reconstructions in this region based on the inverse correlations between tree-ring records and temperature. The inverse correlations between tree-ring records and temperature actually reveal the indirectly correlated effects of temperature on tree growth, which are most likely related to increased moisture stress from evapotranspiration due to higher temperature (Tian et al. 2009, Gao et al. 2013b). Therefore, most of the tree-ring records from the northeastern Tibetan Plateau show responses to the drought or hydroclimatic variations.

In contrast, the tree-ring record in this study shows strong positive correlations with temperatures and no significant ($p < 0.05$) correlations with precipita-

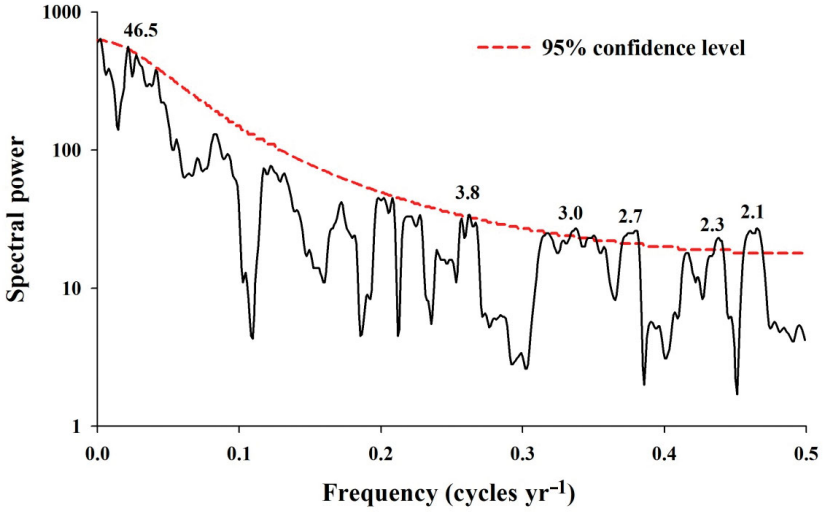

Fig. 6. Spectral analysis using the multi-taper method (MTM), which was performed to evaluate the main spectral properties of the reconstructed July temperature for the period 1785–2009. Values (1/*x*-axis values) above the dashed line are significant at the 95% confidence level

tion (except the preceding December) and PDSI. These results are closely related to the special regional climatic conditions at the study site. The study site is located near a regional rainfall center in the eastern part of the Qilian Mountains, with a total annual precipitation of >500 mm. Therefore, precipitation is likely sufficient here to prevent moisture stress to tree growth. In certain regions with sufficient precipitation and/or very high elevations (Zhu et al. 2008, Zhang et al. 2014), tree-ring records are positively correlated with temperature, and can be used to develop reliable temperature reconstructions.

4.2. Comparisons with other tree-ring based temperature reconstructions

We compared our temperature reconstruction with other tree-ring based temperature reconstructions from the northeastern Tibetan Plateau (Fig. 7). The temperature reconstructions from this region are few and can be summarized by 2 types: (1) warm season temperature reconstructions based on the inverse relationships between tree-ring chronologies and warm season temperatures (Qin et al. 2003, Gou et al. 2008a), and (2) winter temperature reconstructions based on the positive correlations between tree-ring records and winter temperatures (Gou et al. 2007, Liu et al. 2007, Zhu et al. 2008). As our July mean temperature reconstruction belongs to the warm season, we compared our reconstruction with other warm season temperature reconstructions first, and then compared the warm season temperature reconstructions with the winter temperature reconstructions. The warm season temperature reconstructions used in this study for comparisons are the maximum summer half-year (April–September) temperature reconstruction over the past 700 yr using 3 tree-ring chronologies from the Ayemaqin Mountains (Gou et al. 2008a) and the maximum temperature reconstruction (1550–2002) from April through June based on 2 tree-ring series in the southern Qinghai plateau (Qin et al. 2003) (Fig. 7a). The winter temperature reconstructions are the minimum winter half-year (October–April) temperature reconstruction for the past 425 yr in the Xiqing Mountains (Gou et al. 2007); the temperature reconstruction from December through April based on tree-ring width and stable carbon isotope chronologies in the central Qilian Mountains (Liu et al. 2007); and the millennial temperature reconstruction from September through April in the Wulan area (Zhu et al. 2008) (Fig. 7b). All temperature reconstruction series were *z*-transformed and smoothed with an 11 yr fast Fourier transform.

Fig. 7a shows the comparisons of our reconstruction with 2 other warm season temperature reconstructions. The 3 reconstructed temperature series present similar patterns, even though the reconstructions derived from Gou et al. (2008a) and Qin et al. (2003) were based on the negative correlations between tree growth and temperature. Cooling periods were found in all 3 reconstructions in the early 19th century, the late 19th century to the early 20th century, and the 1960s–1970s. Relatively warm periods occurred in the 1820s–1830s, 1920s–1930s, and 1950s, as well as the strikingly warming trend since the 1980s. The winter temperature reconstructions also displayed similar patterns (Fig. 7b), with relatively warm intervals in the 1800s, 1900s, and since the 1980s, and pronounced cooling periods in the 1820s and 1920s. Additionally, the temperature reconstructions from Liu et al. (2007) and Zhu et al. (2008) recorded another relatively warm period in the 1940s.

The temperature reconstruction in this study indicated relatively cold conditions in the eastern Qilian Mountains during the 1890s–1900s and the 1970s–1980s. These 2 cold periods were also indicated by tree-ring records from the western loess plateau in

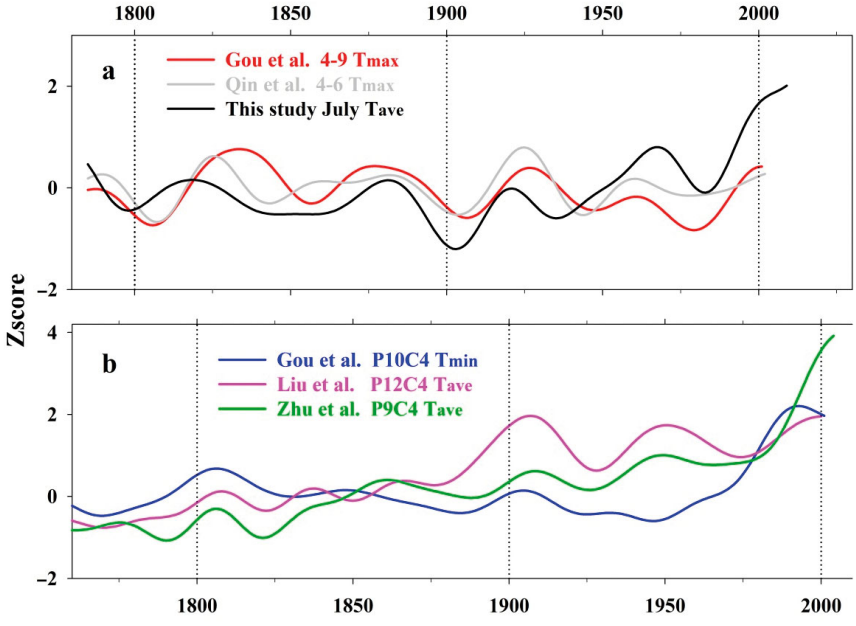

Fig. 7. Comparisons of temperature reconstructions (warm season and winter) from the northeastern Tibetan Plateau. All series were normalized and smoothed with an 11 yr fast Fourier transform function. (a) Warm season maximum temperature reconstructions representing April–September (Gou et al. 2008a), April–July maximum temperature reconstructions (Qin et al. 2003), and the July mean temperature reconstruction (this study). (b) Winter temperature reconstructions extending from October in the previous year to April in the current growth year for the minimum temperature (Gou et al. 2007), from the preceding December to current April for the mean temperature (Liu et al. 2007), and from the preceding September to current April for the mean temperature (Zhu et al. 2008). Note differences in *x*-axis scales between panels

China (Song et al. 2014). The records suggested that these 2 cold periods coincide with the sun activity minimum during 1880–1900 and a slight decrease of sun activity over 1940–1970. Another obvious feature indicated by our temperature reconstruction is that there has been an apparent warming trend since 1900 (Fig. 5), which is also indicated by other tree-ring based temperature reconstructions in China, such as on the northeastern Tibetan Plateau (Liu et al. 2009), the central plains of China (Liu et al. 2014), the southeastern Tibetan Plateau (Deng et al. 2014), and the southeastern areas of China (Duan et al. 2013). Additionally, the 20th century warming in China corresponds closely with the warming recorded by some Northern Hemisphere temperature reconstructions (e.g. D'Arrigo et al. 2006). Under global warming, recent temperature increases in many regions of China have been demonstrated by instrumental records and tree-ring records, which is an important feature of current climate change.

4.3. Asymmetric variability between winter and warm season temperatures

By comparing the warm season temperature reconstructions with the winter temperature reconstructions (Fig. 7), we found that the variation patterns of warm season temperatures and winter temperatures were out of phase, with the winter temperature variations pulling ahead of the warm season temperature by about 20 yr. In a previous study, Gou et al. (2008b) found asymmetric variability between the summer maximum temperatures and the winter minimum temperatures on the basis of 2 tree-ring records from the northeastern Tibetan Plateau. They concluded that the winter minimum temperatures vary about 25 yr earlier compared to the summer maximum temperatures. Here, based on 6 tree-ring records from the northeastern Tibetan Plateau region, we confirm the asymmetric variability between winter and warm season temperatures in this area. In our study, the lag time between winter temperatures and warm season temperature differed slightly from that reported by Gou et al. (2008b), which is closely related with the steps for curve smoothing. In general, the warm season temperature reconstructions from the northeastern Tibetan Plateau region indicated broad spatial correspondence. Moreover, the warm season temperature variability apparently lagged behind the winter temperature changes by about 20 yr. Future studies based on more temperature records are needed to further demonstrate the offset relationships between winter and warm season temperature variances in this area.

5. CONCLUSIONS

Most tree-ring records from the arid and semiarid regions in northwestern China show responses to moisture variation, except for few sampled from high-elevation or humid sites. Here, we present the first tree-ring based July mean temperature recon-

struction from Qinghai spruce over the period 1785–2009 in the eastern Qilian Mountains. The reconstruction indicated an apparent warming trend since the 1900s, which was also recorded by other tree-ring based temperature reconstructions from China. There were no obvious differences in the temperature reconstructions based on positive or inverse relationships between tree growth and temperatures. The warm season temperature reconstructions lagged behind the winter temperature reconstructions by about 20 yr in the northeastern Tibetan Plateau. However, the potential mechanisms of temperature variability in this area are still unclear, and more tree-ring based temperature reconstructions and analyses are needed to clarify them.

Acknowledgements. We thank Prof. Richard H. Waring and Lucas Longway at Oregon State University for assistance with English language and grammatical editing for the manuscript. We thank Zhiqian Zhao, Junde Su, and Zongying Cao for assistance with tree-ring sample collection. We also appreciate valuable comments and suggestions on the manuscript by the Editor and 3 anonymous reviewers. Funding was provided by the National Science Foundation of China (Nos. 41171039 and 41401047) and the Fundamental Research Funds for the Central Universities (lzujbky-2012-134). L.G. and Y.D. are also funded by the China Scholarship Council.

LITERATURE CITED

Chen F, Yuan YJ, Wei WS, Fan ZA and others (2012) Temperature change recorded by tree ring in Jiuquan during the period from June to September in recent 240 years. Arid Zone Res 29:47–54 (in Chinese)

Chen F, Yuan YJ, Wei WS, Zhang RB and others (2013) Tree-ring-based annual precipitation reconstruction for the Hexi Corridor, NW China: consequences for climate history on and beyond the mid-latitude Asian continent. Boreas 42:1008–1021

Cheng B, Zhu Y, Chen FH, Zhang JW, Huang XZ, Yang ML (2004) Relationship between the surface pollen and vegetation in Shiyang river drainage, Northwest China. J Glaciol Geocryol 26:81–88

Cook ER, Kairiukstis LA (1990) Methods of dendrochronology: applications in the environmental sciences. Kluwer, Dordrecht

Cook ER, Krusic PJ, Anchukaitis KJ, Buckley BM, Nakatsuka T, Sano M (2013a) Tree-ring reconstructed summer temperature anomalies for temperate East Asia since 800 CE. Clim Dyn 41:2957–2972

Cook ER, Krusic PJ, Melvin T (2013b) Program RCSigFree: Version 43ptr05. Lamont-Doherty Earth Observatory, Columbia University, Palisades, NY

D'Arrigo R, Wilson R, Jacoby G (2006) On the long-term context for late twentieth century warming. J Geophys Res 111:D03103, doi:10.1029/2005JD006352

Dai AG, Trenberth KE, Qian T (2004) A global dataset of Palmer Drought Severity Index for 1870–2002: relationship with soil moisture and effects of surface warming. J Hydrometeorol 5:1117–1130

Deng Y, Gou XH, Gao LL, Zhao ZQ, Cao ZY, Yang MX (2013) Aridity changes in the eastern Qilian Mountains since AD 1856 reconstructed from tree-rings. Quat Int 80: 379–393

Deng Y, Gou XH, Gao LL, Yang T, Yang MX (2014) Early-summer temperature variations over the past 563 yr inferred from tree rings in the Shaluli Mountains, southeastern Tibet Plateau. Quat Res 81:513–519

Doran PT, Priscu JC, Lyons WB, Walsh JE and others (2002) Antarctic climate cooling and terrestrial ecosystem response. Nature 415:517–520

Duan JP, Zhang QB, Lv LX (2013) Increased variability in cold-season temperature since the 1930s in subtropical China. J Clim 26:4749–4757

Easterling DR, Wehner MF (2009) Is the climate warming or cooling? Geophys Res Lett 36:L08706, doi:10.1029/2009GL037810

Fang K, Gou X, Chen F, Yang M and others (2009) Drought variations in the eastern part of northwest China over the past two centuries: evidence from tree rings. Clim Res 38: 129–135

Fang KY, Gou XH, Chen FH, Cook ER, Li JB, Buckley B, D'Arrigo R (2011) Large-scale precipitation variability over northwest China inferred from tree rings. J Clim 24: 3457–3468

Fritts HC (1976) Tree rings and climate. Academic Press, London

Gao LL, Gou XH, Deng Y, Yang MX, Zhao ZQ, Cao ZY (2013a) Dendroclimatic response of *Picea crassifolia* along an altitudinal gradient in the eastern Qilian Mountains, northwest China. Arct Antarct Alp Res 45:491–499

Gao LL, Gou XH, Deng Y, Liu WH, Yang MX, Zhao ZQ (2013b) Climate–growth analysis of Qilian juniper across an altitudinal gradient in the central Qilian Mountains, northwest China. Trees (Berl) 27:379–388

Gou XH, Chen FH, Jacoby G, Cook ER, Yang MX (2007) Rapid tree growth with respect to the last 400 years in response to climate warming, northeastern Tibetan Plateau. Int J Climatol 27:1497–1503

Gou XH, Peng JF, Chen FH, Yang MX, Levia DF, Li JB (2008a) A dendrochronological analysis of maximum summer half-year temperature variations over the past 700 years on the northeastern Tibetan Plateau. Theor Appl Climatol 93:195–206

Gou XH, Chen FH, Yang MX, Jacoby G, Fang KY, Tian QH, Zhang Y (2008b) Asymmetric variability between maximum and minimum temperatures in Northeastern Tibetan Plateau: evidence from tree rings. Sci China Ser D Earth Sci 51:41–55

Gou XH, Deng Y, Chen FH, Yang MX, Gao LL, Nesje A, Fang KY (2014) Precipitation variations and possible forcing factors on the Northeastern Tibetan Plateau during the last millennium. Quat Res 81:508–512

Holmes RL (1983) Computer-assisted quality control in tree-ring dating and measurement. Tree Ring Bull 43: 69–78

Huffman GJ, Adler RF, Bolvin DT, Gu G and others (2007) The TRMM Multisatellite Precipitation Analysis (TMPA): quasi-global, multiyear, combined-sensor precipitation estimates at fine scales. J Hydrometeorol 8:38–55

IPCC (Intergovernmental Panel on Climate Change) (2013) Summary for Policymakers. In: Stocker TF, Qin D, Plattner GK, Tignor M and others (eds) Climate Change 2013—the physical science basis. Contribution of Work-

ing Group I to the Fifth Assessment Report of the Intergovernmental Panel on Climate Change. Cambridge University Press, Cambridge

Jones PD, Hulme M (1996) Calculating regional climatic time series for temperature and precipitation: methods and illustrations. Int J Climatol 16:361–377

Li JB, Xie SP, Cook ER, Huang G and others (2011) Interdecadal modulation of El Niño amplitude during the past millennium. Nat Clim Change 1:114–118

Liang EY, Shao XM, Liu XH (2009) Annual precipitation variation inferred from tree rings since AD 1770 for the western Qilian Mts., northern Tibetan Plateau. TreeRing Res 65:95–103

Liu XH, Shao XM, Zhao LJ, Qin DH, Chen T, Ren JW (2007) Dendroclimatic temperature record derived from tree-ring width and stable carbon isotope chronologies in the middle Qilian Mountains, China. Arct Antarct Alp Res 39:651–657

Liu Y, An ZS, Linderholm HW, Chen DL and others (2009) Annual temperatures during the last 2485 years in the mid-eastern Tibetan Plateau inferred from tree rings. Sci China Ser D Earth Sci 52:348–359

Liu Y, Sun JY, Song HM, Cai QF, Bao G, Li XX (2010) Tree-ring hydrologic reconstructions for the Heihe River watershed, western China since AD 1430. Water Res 44: 2781–2792

Liu Y, Zhang YH, Song HM, Ma YY, Cai QF, Wang YC (2014) Tree-ring reconstruction of seasonal mean minimum temperature at Mt. Yaoshan, China, since 1873 and its relevance to 20th-century warming. Clim Past Discuss 10:859–894

Mann ME, Lees JM (1996) Robust estimation of background noise and signal detection in climatic time series. Clim Change 33:409–445

Melvin TM, Briffa KR (2008) A 'signal-free' approach to dendroclimatic standardisation. Dendrochronologia 26:71–86

Qin C, Yang B, Burchardt I, Hu XL, Kang XC (2010) Intensified pluvial conditions during the twentieth century in the inland Heihe River Basin in arid northwestern China over the past millennium. Global Planet Change 72:192–200

Qin NS, Shao XM, Shi XH, Jin LY, Zhu XD, Wang QC (2003) Tree-ring chronology in southern Qinghai and its relation to climatic element. Plateau Meteorol 22:445–450

Rinn F (2003) TSAP—Time Series Analysis and Presentation for WIN. TSAP WIN—Professional version. Time series analysis and presentation for dendrochronology and related applications. RinnTech, Heidelberg

Shao XM, Xu Y, Yin ZY, Liang EY, Zhu HF, Wang SZ (2010) Climatic implications of a 3585-year tree-ring width chronology from the northeastern Qinghai-Tibetan Plateau. Quat Sci Rev 29:2111–2122

Song H, Liu Y, Li Q, Gao N, Ma Y, Zhang Y (2014) Tree-ring based May-July temperature reconstruction since AD 1630 on the western Loess Plateau, China. PLoS ONE 9: e93504

Stokes MA, Smiley TL (1968) An introduction to tree-ring dating. University of Chicago Press, Chicago, IL

Sun JY, Liu Y (2012) Tree ring based precipitation reconstruction in the south slope of the middle Qilian Mountains, northeastern Tibetan Plateau, over the last millennium. J Geophys Res 117:D08108, doi: 10.1029/2011JD 017290

Tian QH, Gou XH, Zhang Y, Wang YS, Fan ZX (2009) May-June mean temperature reconstruction over the past 300 years based on tree rings in the Qilian Mountains of the northeastern Tibetan Plateau. IAWA J 30:421–434

Vaughan DG, Marshall GJ, Connolley WM, Parkinson C and others (2003) Recent rapid regional climate warming on the Antarctic Peninsula. Clim Change 60:243–274

Wang BJ, Huang YX, Wang JS, Tao JH (2006) The seasonal distribution and time-varying of the cloud and vapor flux in Qilian Mountain area. Adv Earth Sci 21:948–955 (in Chinese)

Wigley T, Briffa KR, Jones PD (1984) On the average value of correlated time series, with applications in dendroclimatology and hydrometeorology. J Clim Appl Meteorol 23:201–213

Yang B, Qin C, Bräuning A, Burchardt I, Liu JJ (2011) Rainfall history for the Hexi Corridor in the arid northwest China during the past 620 years derived from tree rings. Int J Climatol 31:1166–1176

Zhang Y, Shao XM, Yin ZY, Wang Y (2014) Millennial minimum temperature variations in the Qilian Mountains, China: evidence from tree rings. Clim Past Discuss 10: 341–380

Zhu HF, Zheng YH, Shao XM, Liu XH, Xu Y, Liang EY (2008) Millennial temperature reconstruction based on tree-ring widths of Qilian juniper from Wulan, Qinghai Province, China. Chin Sci Bull 53:3914–3920

Editorial responsibility: Nils Chr. Stenseth, Oslo, Norway

Submitted: June 16, 2014; Accepted: November 3, 2014
Proofs received from author(s): January 29, 2015